

# Synthesis and properties of waterborne polyurethane-based PTMG and PDMS as soft segment

Yang Du<sup>1</sup> · Jingshu Zhang<sup>2</sup> · Chao Zhou<sup>1</sup>

Received: 16 March 2015 / Revised: 7 July 2015 / Accepted: 30 July 2015 /  
Published online: 4 August 2015  
© Springer-Verlag Berlin Heidelberg 2015

**Abstract** Waterborne polyurethanes (WPU) derived from polytetramethylene ether glycol (PTMG), 3-isocyanatomethyl-3,5,5-trimethylcyclohexyl isocyanate, 1,4-butanediol and dimethylolpropionic acid were synthesized. Hydroxyl-terminated polydimethylsiloxane (PDMS) was introduced to replace part of PTMG as soft segment. The effects of  $[-\text{NCO}]/[-\text{OH}]$  ( $R$  value) and PDMS content on structure and properties of WPU were studied using FTIR, thermal analysis, mechanical test, contacting angle testing and scan electron microscopy (SEM). The results revealed that the trend of particles fusion in WPU film decreased with the increment of  $R$  value by SEM photos. The replacement of PTMG by PDMS led to an obvious change in surface properties of films and distinct phase separation was observed by SEM photos when the PDMS content increased. This is the result when the content of PDMS was 2.0 wt% and  $R$  value is 1.2, the film exhibited excellent mechanical properties with the highest elongation at break and improved tensile strength.

## Introduction

Waterborne polymer emulsions that utilize water as the major carrier are a highly important class of materials in the paint and coating industries, especially [1]. The advantages of low viscosities, very little volatile organic compounds (VOCs), reduced flammability, reduced odor and easy application are exhibited by waterborne formulations [2]. As the versatile environmental friendly materials,

---

✉ Chao Zhou  
104655815@qq.com

<sup>1</sup> Engineering Research Center of Synthetic Resin and Special Fiber, Ministry of Education, Changchun University of Technology, Changchun 130012, China

<sup>2</sup> Jilin Province Product Quality Supervision Test Institute, Changchun 130000, China

waterborne polyurethanes (WPU) have gained increasing interest in a broad range of applications owing to their excellent elasticity, abrasion, resistance, flexibility and broad substrate suitability [3–5]. Polyurethanes are composed of alternating soft and hard segment. The soft segment provides elastomeric character to the polymer while the hard segment forms dimensional stability [6]. Because there exists a degree of thermodynamic immiscibility between the hard urethane segments and the soft polyol segments, polyurethane elastomers exhibit microphase separation, which could result in a structure that can be considered as hard segment domains dispersed in soft segment matrix. Due to the presence of two-phase microdomain structure, the molecular structure of polyurethane can be tailored to meet specific property requirement by varying the hard and soft segment length and concentration. Compared with conventional solvent-borne polyurethanes, the waterborne polyurethanes showed insufficient mechanical strength and stiffness. It is reported that the improved mechanical properties can be achieved by organic–inorganic nanocomposites [7, 8] or adjustment of hard and soft segment proportion.

Since the waterborne polyurethane is easy to hydrate due to its molecular chain structure, the water resistance of WPU film is poor. The particular molecular structure of hydroxyl-terminated polydimethylsiloxane (PDMS) endows it with many unique properties, for example low surface tension, resistance to high and low temperatures, excellent flexibility and chemical inertness [9–12]. Therefore, the introduction of PDMS into a polyurethane agent can enhance the hydrophobicity, softness, smoothness and resistance to high and low temperatures of the film, which can increase the commercial and esthetic value of the materials [13–20]. Yen et al. studied the solution properties and membrane surface properties of PDMS-PU blends and found that PDMS can enhance the hydrophobicity properties of WPU membrane effectively [21]. Choi et al. synthesized a novel siloxane–carbonate polyurethane, and found siloxane–carbonate polyurethane has a better phase mixing [22]. Polyurethane elastomers synthesized by PTMG show high modulus and strength, excellent water resistance, abrasion resistance, mold resistance, oil resistant, excellent dynamic mechanical properties, electrical insulation and low temperature flexibility, therefore PTMGs are used in our experiment [23, 24]. Isophorone diisocyanate (IPDI), that is a kind of excellent diisocyanate with the advantages of unfavorable yellow and easy controlling of the reaction condition, can be used to synthesize WPU with relatively simple technical process, and mainly used for polyurethane coating [25, 26].

In this paper, WPUs that derived from polytetramethylene ether glycol (PTMG) 3-isocyanatomethyl-3,5,5-trimethylcyclohexyl isocyanate (IPDI), 1,4-butanediol and dimethylolpropionic acid (DMPA) were synthesized. Hydroxyl-terminated polytetramethylene oxide (PDMS) was introduced to replace part of PTMG as soft segment. Our purpose of the present work is to study the effects of molar ratio of isocyanate and hydroxyl value ( $R$  value) and PDMS content on the structural, thermal and mechanical properties of the polyurethane films.

## Experimental

### Materials

Polytetramethylene ether glycol (PTMG) (purchased from Bayer) as monomer,  $M_n = 2000 \pm 50$  and hydroxyl value 54.7–57.5 mg KOH/g, dihydroxybutyl-terminated polydimethylsiloxane (PDMS) (purchased from Conghua technology Co., LTD,  $M_n = 2000$ ) as modified agent and 1,4-butanediol (BDO, 99.5 wt%) (purchased from Aldrich Chemical) as chain extender were dried under vacuum at 85 °C for 24 h before used. Dimethylolpropionic acid (DMPA) (purchased from Aldrich Chemical, America) was used as hydrophilic chain extender and dissolved in DMAC before used. *N,N*-Dimethylacetamide (DMAC, 99.5 %) and acetone as solvent were purchased from Sinopharm Chemical Reagent Co. Ltd and used as received. Isophorone diisocyanate (IPDI, 99.5 wt% purity, purchased from Bayer) as hard segment was used as received. Dibutyltin dilaurate (DBTDL, 95 %) as catalyst was purchased from Aldrich Chemical. Triethylamine (TEA, 99 wt%) was purchased from Sinopharm Chemical Reagent Co. Ltd.

### Synthesis of waterborne polyurethane dispersions

A series of waterborne polyurethane samples, with different  $[-\text{NCO}]/[-\text{OH}]$  ( $R$  value) or different PDMS content but the same  $R$  value (1.2), were synthesized by prepolymer method as follows: The first step was the formation NCO-terminated polyurethane. PTMG and PDMS as soft segment degassed in a vacuum at 85 °C for 4 h and then were placed in a four-neck, round-bottom flask equipped with a thermometer, mechanical stirrer, condenser with a drying tube, an inlet for dry nitrogen and a heat jacket. The mixture was allowed to 80 °C with moderating stirring 350 rad/min. IPDI was then dropped slowly into the flask, and one droplet DBTDL (0.02 g) was added as catalyst at the same time. After 2 h, DMPA dissolved in DMAC and 1, 4-BDO was added into the flask and the reaction was kept until the theoretical  $-\text{NCO}$  content was reached. In the process, moderate acetone was added to adjust the viscosity of the solution. The next step was the neutralization and emulsifying process. Tertiary amine (TEA) was used as neutralizing agent of the carboxyl group of polyurethane in 45 °C, stirring for 30 min and then emulsions were prepared. The emulsifying process was as follows: distilled water was added to the flask with vigorous stirring 1250 r/min, 30 min. The WPU dispersion was obtained after removal of acetone under vacuum. The synthesis route of WPU is shown in Fig. 1, and the detail recipes in the experiment are listed in Table 1.

### Preparation of WPU latex films

The latex films were prepared by casting the dispersions on a leveled PTFE template under ambient conditions for 24 h and then vacuum drying to a constant weight at 80 °C for 24 h. The films with thickness range 200  $\mu\text{m}$ –1 mm were prepared for the use of further investigation.

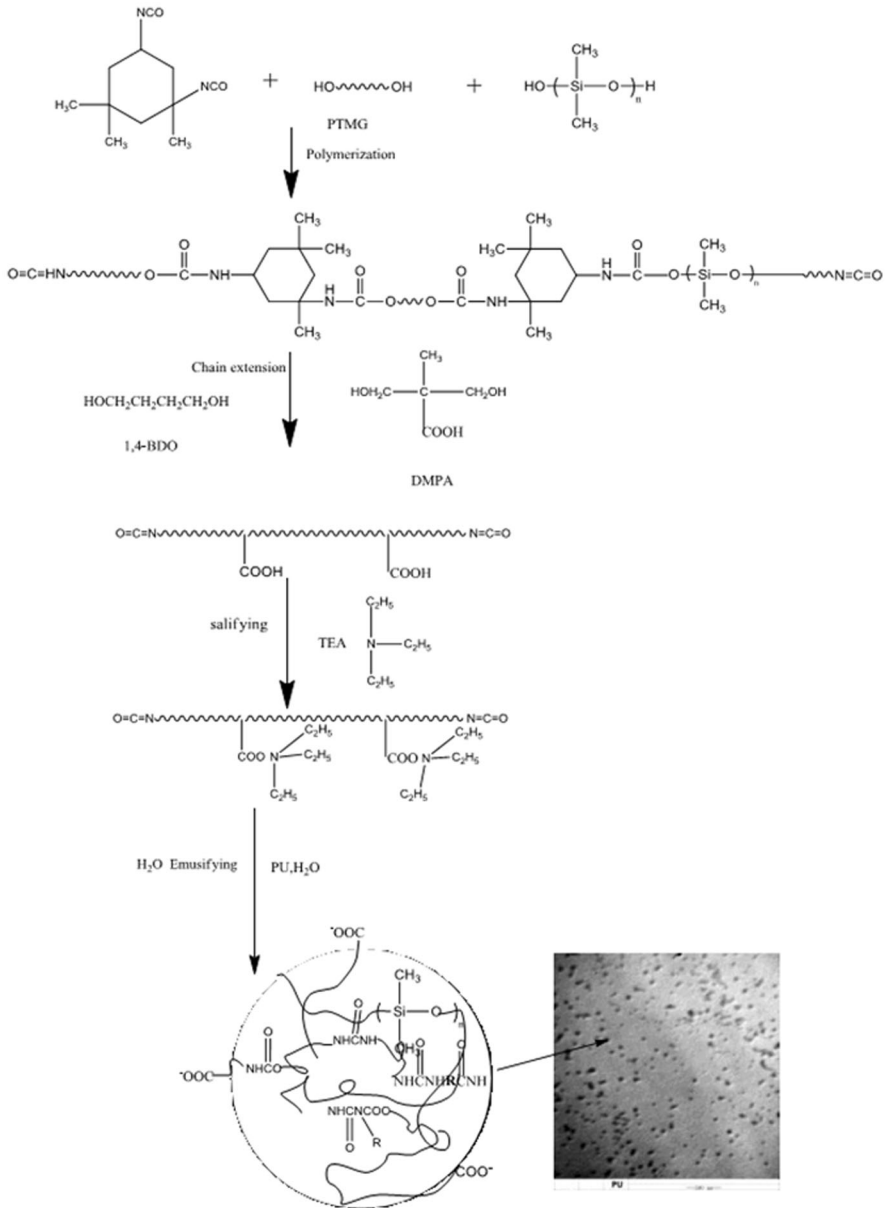


**Fig. 1** Synthesis route of waterborne polyurethane

## Characterization

Infrared spectra of the WPU films samples were recorded on a Nicolet IS50 Fourier-transform infrared spectrometer in ATR mode over 64 scans with a resolution of  $8\text{ cm}^{-1}$ . The average particle size and the particle size distribution of emulsion were

**Table 1** Recipes for the preparation of waterborne polyurethane

Sample	Ingredient				
	IPDI/g	PTMG/g	PDMS/g	PDMS wt%	R value
PU0	25.3	40.0	0	0	1.2
PU1	25.5	40.0	1.45	2	1.2
PU2	29.5	40.0	1.45	2	1.4
PU3	34.0	40.0	1.45	2	1.6
PU4	37.0	40.0	1.45	2	1.8
PU5	25.5	38.5	3.00	4	1.2
PU6	25.5	37.0	4.50	6	1.2
PU7	25.5	35.5	6.00	8	1.2
PU8	25.5	34.0	7.50	10	1.2
PU9	25.5	31.3	10.2	15	1.2
PU10	25.5	25.8	15.5	20	1.2

measured by dynamic light scattering that carried out on Brookhaven 90 plus Particle Size Analyzer at 25 °C, and the samples were highly diluted to prevent multiple scattering before test. Surface tension of emulsion was measured by plate method using surface tension meter (Shanghai Equity Instrument Factory, BZY-1) at 25 °C. Dynamic mechanical analysis (DMA) measurements were carried out on a viscoelastometer (Perkin Elmer Company) with temperature range from –100 °C to 100 °C at 10 Hz. The heating rate was 5 °C/min, and the dimension of the sample was 4 mm × 20 mm × 0.5 mm. Thermogravimetric analysis (TGA) was carried out with Pyris 1TGA thermogravimetric analyzer (Perkin Elmer) at a heating rate of 10 °C/min in nitrogen atmosphere, temperature ranging from ambient temperature to 600 °C. The contact angle, which is a measure of the surface wettability, was used to determine the hydrophobicity and hydrophobicity. The contact angles of water and ethylene glycol were measured at 25 °C using a contact angle goniometer (DSA30, Kruss Company). The contact angle values reported are averages of three measurements that taken at three different location of the film. Mechanical testing was carried out on a tensile tester (Instron 3365, USA) at room temperature with a speed of 300 mm/min. All measurements have an average of three runs. All tensile specimens were molded into a dumbbell type whose dimensions in the parallel part were 30 mm in length. Scanning electron microscope (JSM-6510) with 10 kV accelerating voltage was used to observe the cross sections of fractured WPU films. The cross sections were coated with gold before SEM observation.

## Results and discussion

### FTIR analysis

Figure 2 shows FTIR-IR spectra of WPU samples. The characteristic bands at approximately 1700, 1100–1110 and 3330  $\text{cm}^{-1}$  confirm the carbonyl group of

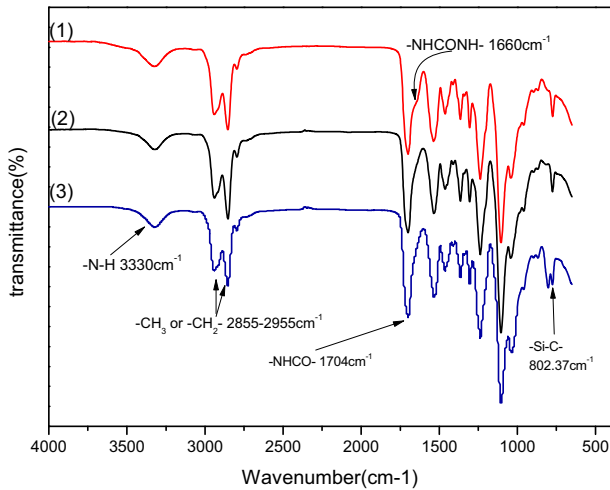


**Fig. 2** FTIR spectra of WPU / PU4,  $R = 1.6$ , PDMS 2 wt%, 2 PU0,  $R = 1.2$ , PDMS 0 wt%, 3 PU9,  $R = 1.2$ , PDMS 20 wt%

urethane, ether (C–O–C) group and amino group in these samples, respectively [27, 28]. Comparing Fig. 2(1, 2), absorption peak intensity of urea carbonyl at  $1660\text{ cm}^{-1}$  (–NHCONH–) increases with  $R$  value from 1.2 to 1.6, which is due to isocyanate and water extender chain or the urethane further reaction. Comparing Fig. 2(2, 3), it can be found that characteristic absorption peak of –Si–CH<sub>3</sub> and –Si–O– appeared at 802.37 and  $1033\text{ cm}^{-1}$ , which indicates that the PDMS has accessed of polymer chain successfully.

The FTIR spectra is analyzed using a curve resolving technique based on linear least-squares analysis to fit the combination of Lorentzian and Gaussian curve shapes. Figure 3 shows the curve fitting of the carbonyl group of urethane (–NH–(C=O)–) and the carbonyl group of uramido (–NH–(C=O)–NH–).  $1704\text{ cm}^{-1}$  is the carbonyl absorption peak in –NHCO–, and  $1660\text{ cm}^{-1}$  is urea carbonyl absorption peak (–NHCONH–). It can be seen that characteristic absorption peaks of the urea carbonyl groups in  $1660\text{ cm}^{-1}$  gradually become strong with the increment of  $R$  value, which is caused by the reaction of residual isocyanate with water resulting in the extension of chain.

Figure 4 shows the FTIR spectra of WPU with different PDMS content. As shown in Fig. 4(1), the peak of  $802.37\text{ cm}^{-1}$  presents the characteristic absorption of –Si–CH<sub>3</sub>. The curves indicate that the intensity of infrared absorption peak gradually increases with PDMS content. Furthermore, it is found that the intensity of  $1033\text{ cm}^{-1}$  (–Si–O–) increased with the PDMS content shown in Fig. 4(2).

### The properties of WPU emulsion

Physical properties of emulsion also have important influence on film-forming process and film properties. Table 2 lists physical properties of WPU emulsion. The

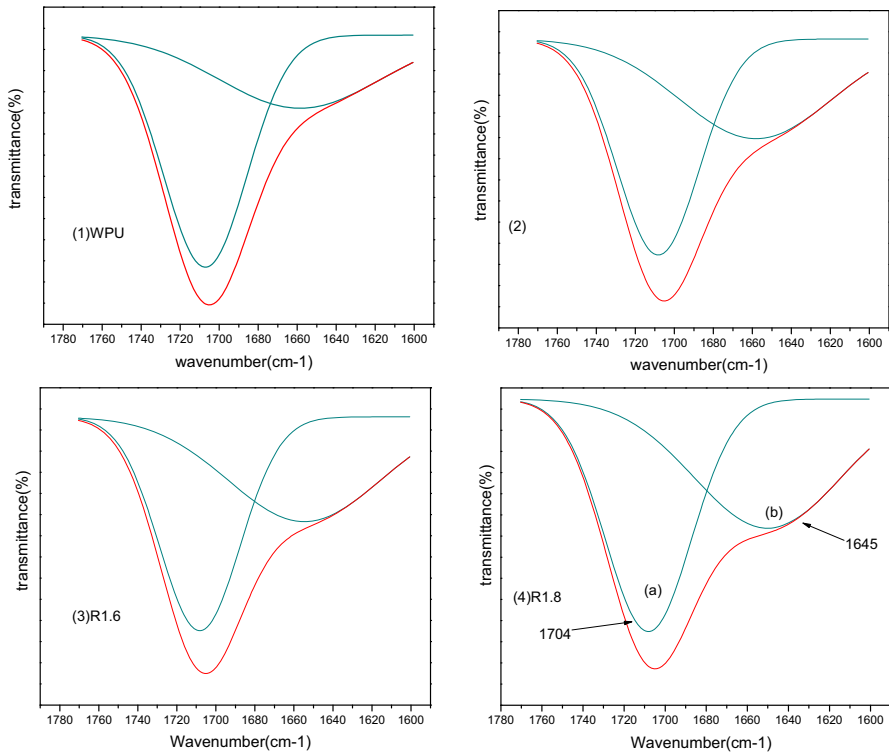


**Fig. 3** Decomposition of *a* carbonyl ( $-\text{NH}-(\text{C}=\text{O})-$ ) and *b* carbonyl ( $-\text{NH}-(\text{C}=\text{O})-\text{NH}-$ )

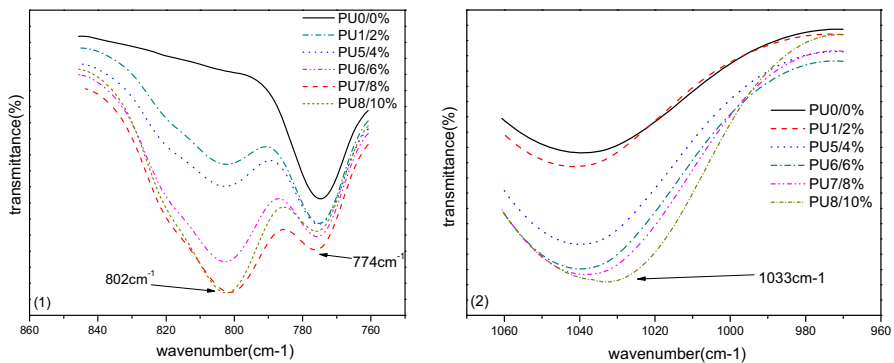


**Fig. 4** FTIR spectra of WPU film in different content of PDMS study

particle size and particle size polydispersity index (PDI) were measured by dynamic light scattering, and the surface tension was measured by the abruption method. As shown the particle size of emulsion increases with *R* value. And as the *R* value reaches 1.6, the particle size rise up to 200 nm and emulsion appearance is milk

**Table 2** The physical properties of emulsions

Sample	PDMS wt%	<i>R</i> value	Particle size (nm)	Polydispersity index (PDI)	Surface tension (mN/m)	Emulsion appearance
PU0	0	1.2	44.9	0.067	38.0	Transparent
PU1	2	1.2	51.8	0.097	31.7	Transparent
PU2	2	1.4	89.0	0.140	30.3	Sub-transparent
PU3	2	1.6	217.2	0.224	29.1	Milk white
PU4	2	1.8	243.3	0.237	24.0	Milk white
PU5	4	1.2	48.1	0.156	23.9	Transparent
PU6	6	1.2	55.0	0.168	23.7	Transparent
PU7	8	1.2	57.0	0.177	21.8	Transparent
PU8	10	1.2	65.4	0.233	27.1	Transparent
PU9	15	1.2	58.9	0.243	28.2	Transparent
PU10	20	1.2	82.3	0.270	28.1	Sub-transparent

white. This phenomenon may be explained as follows: the increment of *R* value leads to the increase of hard segment proportion and the chain of macromolecule is not easy to curl.

According to the Brown's formula of the film-forming conditions [29] :

$$G \leq 35(\gamma)/R,$$

where  $\gamma$  is the surface tension of the polymer–water interface, *R* is the radius of the polymer spheres, and *G* is the capillary forces. The smaller and more soft the particle size, the better the film performance, but the worse water resistance.

The decrement of the emulsion surface tension is found with increment of *R* value, which is beneficial to spreading property and film-forming properties of emulsion. Furthermore, due to the effect of PDMS content on the properties of WPU emulsion, it can be found that PDMS content has less effect on the latex particle diameter, but great influence on the polydispersity index (PDI) of emulsion that described the distribution of latex particle size, which changes from 0.067 to 0.237. And the surface tension of the emulsion decreased to reach a minimum 21.8 mN/m with PDMS content 8 wt%.

### DMA and TGA analysis of WPU films

Generally, polyurethane has two phases: soft segment and hard segment. DMA curves of PU always give two  $\tan\delta$ : One belongs to soft segment in lower temperature; the other belongs to hard segment phases in higher temperature. In our study, since the  $T_g$  of hard segment of PU is close to the viscous flow temperature, only the  $T_g$  of soft segment is discussed. Figure 5 shows the DMA curve of WPU with different *R* value. It can be found when the *R* value increases from 1.2 to 1.8, the glass transition temperature of the soft segment phase decreases from  $-65$  to  $-72$  °C. This may be due to the significant phase separation caused by increasing of the hard segments content because if microphase interval fusion is better, the glass



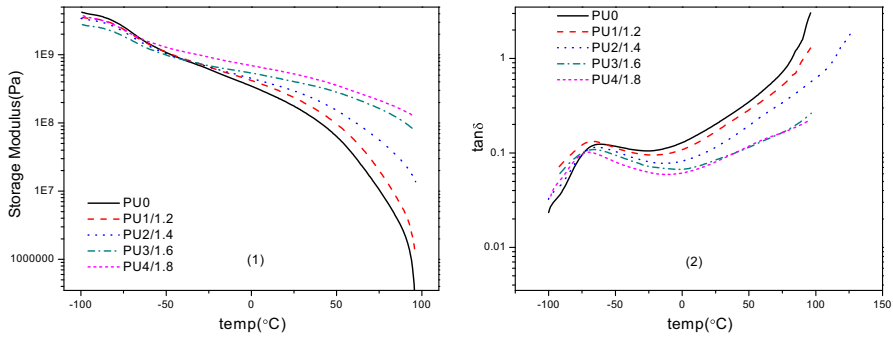
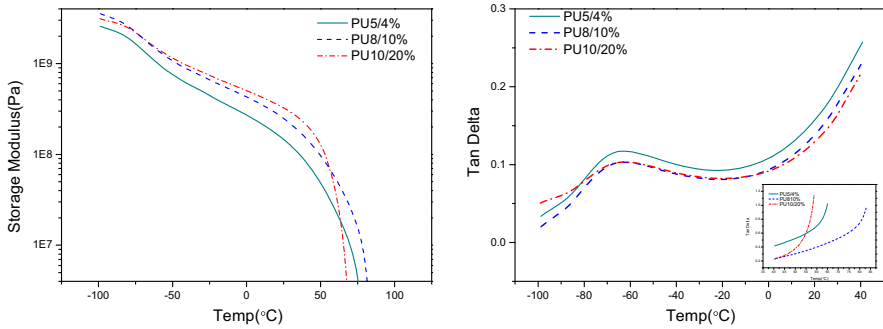


**Fig. 5** DMA curves of WPU films with different  $R$  value

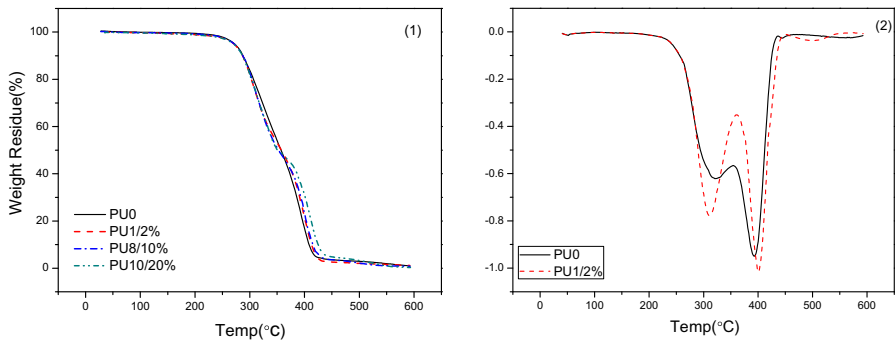
transition temperature of two phases should be closer. Figure 5(1) also shows the storage modulus and temperature curves of WPU with different  $R$  value. It shows that below approximately  $-40$  °C, the WPU film sample with  $R$  value 1.2 shows the highest storage modulus. However, above approximately  $-40$  °C, the storage modulus increases with  $R$  value, and WPU sample with  $R$  value 1.8 has the higher storage modulus. Hard segment in PU chain provides film with mechanical properties at high temperature region, so the increment of  $R$  value leads to the increasing of storage modulus. Figure 5(2) shows the internal friction vs temperature curves of samples, the internal friction increases with the temperature increasing at low temperature, and the high temperature zone is on the contrary.

Figure 6 shows DMA curves of WPU with different PDMS content. It shows that increase of PDMS content leads to an increase of storage modulus of the film but has less effect on the  $T_g$  of soft segment. Furthermore, it can be found that increasing the PDMS content in the soft segment accelerates the arrival of viscous flow of WPU.

To examine the effect of PDMS on the thermal stability, thermogravimetric analysis (TGA) is carried out and the results are shown in Fig. 7(1), and Fig. 7(2) is TGA signal for the first derivative of the temperature curve [30–32]. The results show that there appears to be a platform region after introduction of PDMS, and WPU films with PDMS have a lower degradation temperature when temperature is less than 375 °C, but above 375 °C the films have a higher degradation temperature. The onset of the first step is around 250 °C and completed around 375 °C which corresponds to produce the starting materials such as diisocyanate, polyol and some side products, the fastest temperature of degradation is around 310 °C is the boiling point of IPDI. The second stage of degradation corresponds to that chain scission of polyol such as PTMG occurs at about 400 °C and produces more volatile chain fragments and rearrangement products, which started at 375 °C and ended at about 430 °C in Fig. 7(2). Two degradation stages are more obvious after the introduction of PDMS in Fig. 7(2). Table 3 shows the temperature of 70 % weight loss of WPU film. When increasing PDMS content to 20 wt%, the temperature increases from 385.03 to 400.23 °C. This suggests that the introduction of PDMS can increase the thermal stability of WPU films to a certain extent.



**Fig. 6** DMA curves of WPU films with different PDMS content



**Fig. 7** TGA and DTG curves of WPU with different PDMS content

**Table 3** TGA properties of WPU films

Sample	PU0 (without PDMS)	PU0 (2 % wt PDMS)	PU0 (10 % wt PDMS)	PU0 (20 % wt PDMS)
70 % weight loss temp (°C)	385.03	390.21	392.45	400.23

### Contact angle and surface-free energy of WPU with different PDMS content

The hydrophobicity of the PDMS-modified polyurethane films was investigated through the static contact angle. The surface-free energy was also calculated from contact angle values. Using the Owens and Wendt equation as follows: [33]:

$$\gamma_s = \gamma_s^d + \gamma_s^p$$

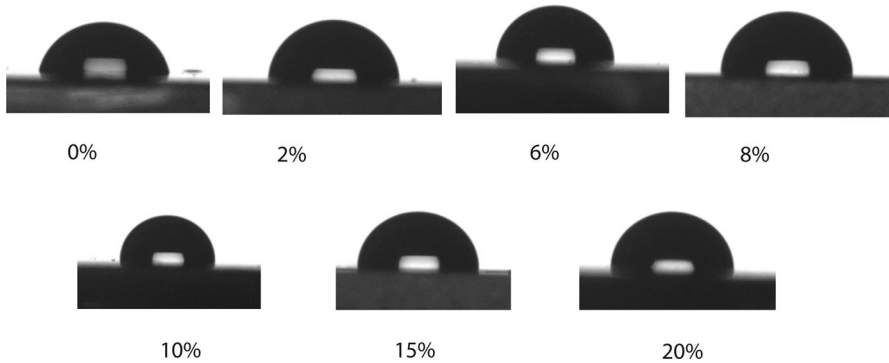


**Fig. 8** Water droplets on the surface of WPU films with different PDMS content

$$\gamma_L(1 + \cos\theta) = 4 \left( \frac{\gamma_S^d \gamma_L^d}{\gamma_S^d + \gamma_L^d} + \frac{\gamma_S^p \gamma_L^p}{\gamma_S^p + \gamma_L^p} \right),$$

where  $\theta$  is the contact angle of liquid on the surface of materials,  $\gamma_L$  is the surface tension of the liquid,  $\gamma_L^d$  and  $\gamma_L^p$  are the dispersion and polar components of the liquids, and  $\gamma_S^p$  and  $\gamma_S^d$  are the polar and dispersion component of the solids. Dispersion component and polar component of water are 21.8 and 51.0 mJ/m<sup>2</sup>, and ethylene glycols’ are 29.3 and 19.0 mJ/m<sup>2</sup>, respectively.

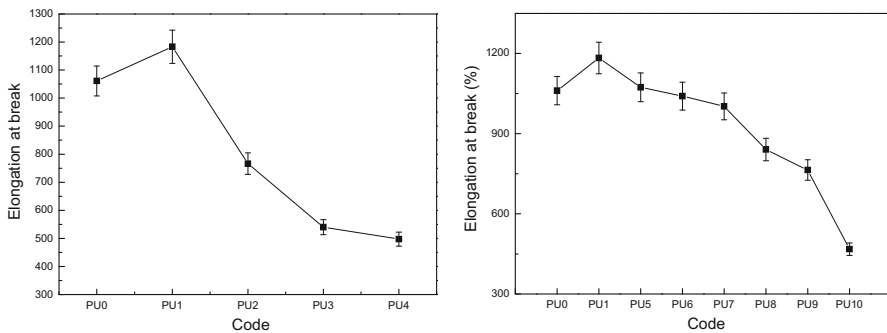
The static contact angle and surface-free energy values are given in Table 4. The water contact angle increased with the PDMS content and reached the maximum 92.1° at PDMS content of 10 wt% (Fig. 8). A small amount of PDMS can improve the contact angle with water of polyurethane films, which increased from 76.5° (0 %) to 86.6° (2 %). This may be caused by the enrichment of PDMS on the surface of films. The surface-free energy is an important physical parameter. The surface-free energy decreased with the increasing of PDMS content, but the surface-free energy is stable when the content of PDMS is greater than 15 %. Surface-free energy reaches the minimum of 28.64 mJ/m<sup>2</sup> when the PDMS content is 10 %.

**Mechanical properties and stress–strain curves of PU films**

Figure 9(1) shows the elongation at break curves of polyurethane film with different  $R$  value. It can be found that the elongation at break of WPU film reaches a maximum of 1190 % when the  $R$  value is 1.2, and the elongation at break decreases from 1190 to 467 % with the increase of  $R$  value. This is because the  $R$  value responds to the ratio of soft and hard segment so that the harder segment, the greater strength, and the elongation at break decreases accordingly. Table 5 shows that breaking strength and yield strength of the samples increase with the increment of  $R$  value, and elongation after breaking is 183 %. Figure 9(2) shows the elongation at break curves of WPU film with different PDMS content. In the figure, a small amount of PDMS can effectively improve the tensile properties of the material.

**Table 4** Contact angle and surface-free energy values for WPU films

Codes	PDMSwt%	Static contact angle (deg)		Surface-free energy (mJ/m <sup>2</sup> )		
		H <sub>2</sub> O	(CH <sub>2</sub> OH) <sub>2</sub>	$r_s^p$	$r_s^d$	$r_s^i$
PU0	0	76.5	56.0	13.36	19.61	32.97
PU1	2	86.6	57.2	19.39	10.95	30.34
PU5	4	87.1	57.9	19.23	10.78	30.01
PU6	6	87.9	58.5	19.47	10.31	29.78
PU7	8	88.1	60.5	17.84	10.92	28.76
PU8	10	92.1	62.0	20.61	8.03	28.64
PU9	15	87.1	59.5	17.81	11.40	29.21
PU10	20	87.1	59.3	17.98	11.32	29.3

**Fig. 9** The elongation at break of different WPU films (Note: the tensile rate 300 mm/min)**Table 5** Yield strength, breaking strength and elongation after breaking of WPU films

Codes	PU0	PU1	PU2	PU3	PU4	PU5	PU6	PU7	PU8	PU9	PU10
Yield strength (MPa)	3.7	4.0	7.5	12.0	14.3	4.97	7.3	11.3	5.3	6.1	8.7
Breaking strength (MPa)	13.0	15.2	33.2	34.4	35.0	41.0	48.5	28.5	32.1	26.1	18.0
Elongation after breaking (%)	283	183	183	183	183	183	183	183	183	183	183

When the PDMS content is 2 wt%, the film gained a maximum elongation at break. However, the high content of PDMS replacing PTMG can lead to significantly reduce the elongation. Table 5 shows that breaking strength of the sample with PDMS content 6 % is the maximum 48.5 MPa, and the yield strength of the PDMS content of 8 % is the maximum 11.3 MPa.

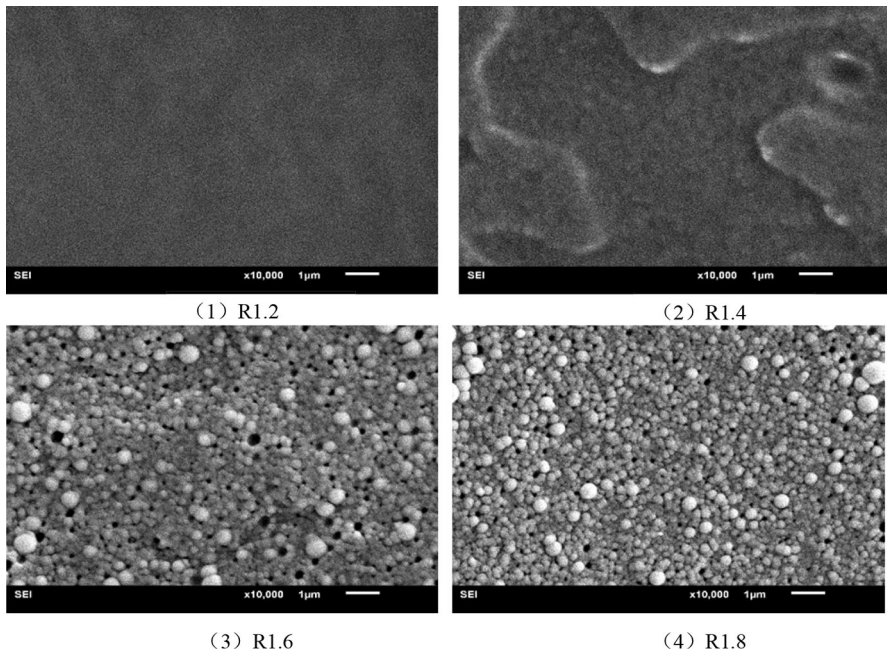


**Fig. 10** SEM images of cross sections of WPU film with different  $R$  value

### SEM images of cross sections of WPU films

Scanning electron microscope was employed to investigate the morphology of WPU film. Figure 10 shows graphs of cross sections of WPU films with different  $R$  value. It can be seen that the polyurethane particles show clearly the increasing of  $R$  value and meanwhile particle fusion effect becomes poorer. Figure 10(1) shows that particles have good fusion, the section is substantially uniform, but Fig. 10(2) has obviously become rough. Figure 10(3, 4) shows the particle size of about 250 nm that agrees with the data obtained from the light scattering. Increasing the  $R$  value leads to the increment of hard segment proportion, which causes the hardness of particles and the fusion degree is suppressed. It leads ultimately to changes in the mechanical properties of the film.

Figure 11 shows SEM images of WPU films with different PDMS content but same  $R$  value (1.2). When no PDMS was introduced in the WPU (Fig. 11(1)), the section shows smooth and no phase separation is observed. Phase separation becomes remarkable as shown in Fig. 11 when the PDMS was introduced and its content increases from 2 to 20 %. Figure 11(2–4) shows an unequal size distribution of phase microdomains, but these spots (1–4  $\mu\text{m}$ ) have the same morphologies. The phenomenon suggests a higher incompatibility between PDMS soft segment, other soft segment and hard segment. So the mechanical properties of the material are obviously different.

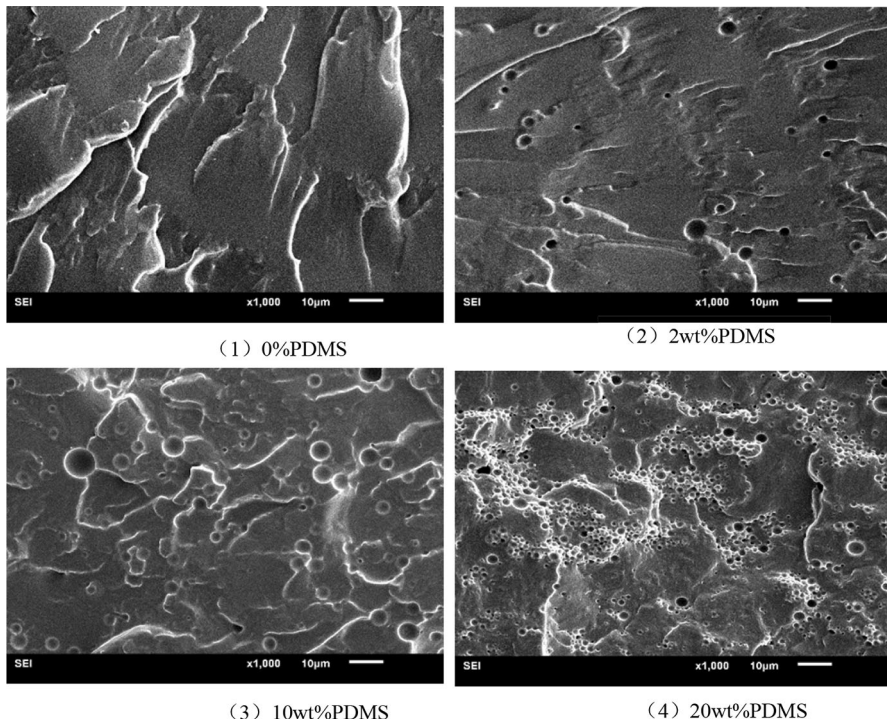


**Fig. 11** SEM images of cross sections of WPU films with different PDMS content

## Conclusions

A series of WPU emulsion with different  $R$  value and PDMS content were synthesized, and the basic physical properties of emulsion and the mechanical properties of films material were investigated. The results showed that increment of  $R$  value lead to the increasing of emulsion particle size, polydispersity index and storage modulus but sacrificing the flexibility of the film. SEM results showed that particle fusion becomes worse with the increment of  $R$  value. Hydroxyl-terminated PDMS replaced polyether polyol to react with isocyanate, and accessed to the polymer chain. The tensile strength was increased, the elongation at break was decreased and decomposition properties were better at high temperature with the increment of PDMS content. The study on properties of film material surface showed that film with 10 % PDMS have a maximum of water contact angle, while the surface energy was reduced at the same time. SEM results showed that obvious phase separation occurred with the increment of PDMS content. This was mainly due to a higher incompatibility between the PDMS chains and hard segment because of the differences in chemical structure. Effect of  $R$  value is greater than PDMS content on physical and mechanical properties. When the content of PDMS was 2.0 wt% and 1.2  $R$  value, the film exhibited excellent mechanical properties with the highest elongation (1143 %) at break. As a result of WPU as no pollution and

excellent mechanical properties, it can be used as a solvent polyurethane leather finishing agent of alternative or complementary.

**Acknowledgments** We would like to express our great thanks to the Jilin Province science and technology research and development program of China (20130206071GX) for the financial support.

## References

1. Weiss KD (1997) Paint and coatings: a mature industry in transition. *Prog Polym Sci* 22:203–245
2. Lu Y, Xia Y, Larock RC (2011) Surfactant-free core-shell hybrid latexes from soybean oil-based waterborne polyurethanes and poly (styrene-butyl acrylate). *Prog Org Coat* 71:336–342
3. Rahman MM, Lee WK (2009) Properties of isocyanate-reactive waterborne polyurethane adhesives: effect of cure reaction with various polyol and chain extender content. *J Appl Polym Sci* 114:3767–3773
4. Rahman MM, Kim HD, Lee WK (2009) Properties of waterborne polyurethane adhesives: effect of chain extender and polyol content. *J Adhes Sci Technol* 23:177–193
5. Du H, Zhao Y, Li Q (2008) Synthesis and characterization of waterborne polyurethane adhesive from MDI and HDI. *J Appl Polym Sci* 110:1396–1402
6. Lei L, Zhong L, Lin X (2014) Synthesis and characterization of waterborne polyurethane dispersions with different chain extenders for potential application in waterborne ink. *Chem Eng J* 253:518–525
7. Soares RR, Carone C, Einloft S (2014) Synthesis and characterization of waterborne polyurethane/ZnO composites. *Polym Bull* 71:829–838
8. Zhang S, Yu A, Liu S (2012) Effect of silica nanoparticles on structure and properties of waterborne UV-curable polyurethane nanocomposites. *Polym Bull* 68:1469–1482
9. Pei X, Chen G, Fang X (2013) Synthesis and properties of poly (imide siloxane) block copolymers with different block lengths. *J Appl Polym Sci* 129:3718–3727
10. Sun F, Jiang SL, Liu J (2007) Study on cationic photopolymerization reaction of epoxy polysiloxane. *Nucl Instrum Methods B* 264:318–322
11. Sun F, Jiang SL (2007) Synthesis and characterization of photosensitive polysiloxane. *Nucl Instrum Methods B* 254:125–130
12. He WD, Pan CY (2001) Influence of reaction between second monomer and vinyl group of seed polysiloxane on seeded emulsion polymerization. *J Appl Polym Sci* 80:2752–2758
13. Subramani S, Lee JM, Cheong IW (2005) Synthesis and characterization of water-borne crosslinked silylated polyurethane dispersions. *J Appl Polym Sci* 98:620–631
14. Wang LF, Ji Q, Glass TE (2000) Synthesis and characterization of organosiloxane modified segmented polyether polyurethanes. *Polymer* 41:5083–5093
15. Rhodes NP, Bellón JM, Buján MJ (2005) Inflammatory response to a novel series of siloxane-crosslinked polyurethane elastomers having controlled biodegradation. *J Mater Sci-Mater M* 16:1207–1211
16. Ni H, Johnson AH, Soucek MD (2002) Polyurethane/polysiloxane ceramer coatings: evaluation of corrosion protection. *Macromol Mater Eng* 287:470–479
17. Pieper RJ, Ekin A, Webster DC (2007) Combinatorial approach to study the effect of acrylic polyol composition on the properties of crosslinked siloxane-polyurethane fouling-release coatings. *J Coat Technol Res* 4:453–461
18. Sommer SA, Byrom JR, Fischer HD (2011) Effects of pigmentation on siloxane-polyurethane coatings and their performance as fouling-release marine coatings. *J J Coat Technol Res* 8:661–670
19. Holmes-Farley SR, Minichelli JL (1991) The mechanism of cure initiation of a surface-activated adhesive. *J Adhes Sci Technol* 5:409–420
20. Holmes-Farley SR, Yanyo LC (1990) Thin anisotropic coatings based on sol-gel technology. In: *MRS Proceedings*, vol 180. Cambridge University Press, p 439
21. Yen MS, Tsai PY, Hong PD (2006) The solution properties and membrane properties of polydimethylsiloxane waterborne polyurethane blended with the waterborne polyurethanes of various kinds of soft segments. *Colloid Surf A* 279:1–9
22. Choi T, Masser KA, Moore E (2011) Segmented polyurethanes derived from novel siloxane-carbonate soft segments for biomedical applications. *J Polym Sci Polym Phys* 49:865–872

23. Daemi H, Barikani M, Barmar M (2013) Compatible compositions based on aqueous polyurethane dispersions and sodium alginate. *Carbohydr Polym* 92:490–496
24. Li Y, Pan D, Chen S (2013) In situ polymerization and mechanical, thermal properties of polyurethane/graphene oxide/epoxy nanocomposites. *Mater Des* 47:850–856
25. Jinghui W, Yao Y (2012) The synthesis and property of IPDI-based waterborne polyurethane elastic membrane. *Polyurethane Ind* 1:008
26. Guo Y, Guo J, Li S (2013) Properties and paper sizing application of waterborne polyurethane emulsions synthesized with TDI and IPDI. *Colloid Surf A* 427:53–61
27. Sadtler Research Laboratories (1978) Sadtler handbook of infrared spectra
28. Datta J, Kacprzyk M (2008) Thermal analysis and static strength of polyurethanes obtained from glycolysates. *J Therm Anal Calorim* 93:753–757
29. Wilson AD, Prosser H (1991) *Waterborne coatings*. Springer Science & Business Media, pp 117–118
30. Datta J (2010) Synthesis and investigation of glycolysates and obtained polyurethane elastomers. *J Elastom Plast* 42:117–127
31. Datta J, Rohn M (2007) Thermal properties of polyurethanes synthesized using waste polyurethane foam glycolysates. *J Therm Anal Calorim* 88:437–440
32. Datta J, Pasternak S (2005) Oligourethane glycols obtained in glycolysis of polyurethane foam as semi-finished products for cast urethane elastomers preparation. *Polimery* 50:352–357
33. Wu SH (1982) *Polymer interface and adhesion*. Marcel Dekker Inc, New York, pp 178–181